This is a repository copy of *Compressive Sensing Based Approach to the Design of Linear Robust Sparse Antenna Arrays with Physical Size Constraint*.

Article:

Compressive Sensing Based Approach to the Design of Linear Robust Sparse Antenna Arrays with Physical Size Constraint

Matthew B. Hawes and Wei Liu

Communications Research Group

Department of Electronic and Electrical Engineering

University of Sheffield, S1 3JD

United Kingdom

{elp10mbh, w.liu}@sheffield.ac.uk

January 8, 2014

Abstract. In sparse arrays, the randomness of antenna locations avoids the introduction of grating lobes, while allowing adjacent antenna spacings to be greater than half a wavelength. This means a larger array size can be implemented using a relatively small number of antennas. However, careful consideration has to be given to antenna locations to ensure that an acceptable performance level is achieved. Model perturbations can also cause steering vector errors, which in turn cause discrepancies in the array's response, making robust arrays desirable. This paper presents various compressive sensing based methods that can solve this problem, while also imposing the antenna size as a constraint on the minimum adjacent antenna separations. Narrowband and multiband design examples are presented to verify the effectiveness of the proposed design methods, with comparisons being drawn with a previously proposed genetic algorithm based approach.

Keywords. Sparse array, robust beamforming, compressive sensing, size constraint, location optimization.

1 Introduction

For Uniform Linear Arrays (ULAs), the adjacent antenna spacing has to be no larger than $\lambda/2$ (λ is the wavelength of interest) in order to avoid unwanted grating lobes [1, 2, 3, 4]. This can be problematic when considering arrays with a large aperture size, due to the cost associated with the number of antennas required. As a result, sparse arrays are a desirable alternative [5]. The non-uniform nature of sparse arrays can avoid grating lobes while allowing adjacent antenna separations greater than $\lambda/2$, meaning an array of a given aperture size can be achieved with less antennas.

However, the tradeoff in using sparse arrays is their unpredictable sidelobe behaviour. As a result it is often necessary to optimise the antenna locations in order to achieve a desired performance, e.g. minimising the peak sidelobe level. Some nonlinear optimisation methods such as Genetic Algorithms (GAs) [6, 7, 8, 9, 10], and Simulated Annealing (SA)[11], have been regularly used to achieve this required optimisation. Difference sets and almost difference sets have also been successfully used in the design of sparse arrays, [12, 13], and merged with GAs to help give an improved performance, [14, 15]. The disadvantage of GAs, and similar design methods, is the potentially long computation time and the possibility of convergence to a non-optimal solution.

More recently, the area of Compressive Sensing (CS) has been explored [16], and CS-based methods have been proposed in the design of sparse arrays [17, 18, 19, 20, 21, 22]. CS theory tells us that when certain conditions are met it is possible to recover some signals from fewer measurements than used by traditional methods [16]. This can then form the basis of sparse array design methods by trying to get an exact, or almost exact, match to a reference pattern while using as few sensors/antennas as possible. Alternatively, the problem could be converted into a probabilistic framework and solved using a relevance vector machine [23]. This approach has been used in the design of sparse arrays with real valued and complex valued weight coefficients [24, 25, 26]. Further work has also shown that it is possible to improve the sparseness of a solution by considering a reweighted l_1 minimisation problem [27, 28, 29]. The aim of these methods is to bring the minimisation of the l_1 norm of the weight coefficients closer to that of the minimisation of the l_0 norm. To do this an iterative method is required to solve a series of reweighted l_1 minimisation problems, where locations with small weight coefficients are more heavily penalised than locations with large weight coefficients.

Previous work using CS to design sparse arrays has mainly focused on the traditional beamforming scenario, where the steering vector of the array is known exactly. In practice, this may not always be the case, as there are various possible model perturbations, such as errors in antenna locations, mutual coupling and discrepancies in individual antenna responses. If one or more of these are present, there will be an error associated with the array's steering vector, which in turn affects the array's response. As a result it is desirable to have an array that is robust to the mismatch between designed and achieved steering vectors.

Various methods have been used to design robust adaptive beamformers, such as diagonal loading, worst case optimisation and robust Capon beamformers [30, 31, 32, 33, 34, 35, 36], where it is usually assumed that there is a norm-bounded steering vector error. In this paper this idea is used to place an extra constraint on the CS-based design process. As a result, the difference between the designed and achieved array responses can be kept below an acceptable level.

It is also possible that the resulting antenna locations will be too close for the antennas to physically fit in, especially for multiband or wideband arrays where sizes may be much larger than $\lambda/2$ [37] . As a result, a constraint of the antennas' physical size has to be considered in the design process and three methods of doing so are proposed in this paper: a straightforward method is to merge locations that are closer together than the size constraint; the second solution is to iteratively solve the problem by incorporating the size constraint in
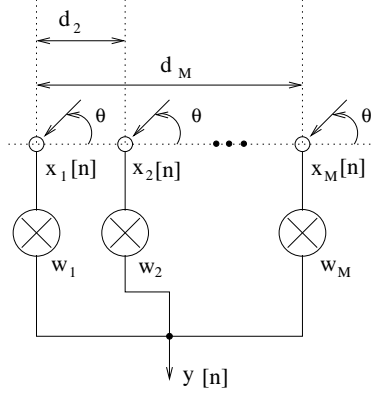
Figure 1: A general narrowband array structure.

the CS process and the third one is based on an altered reweighting scheme.

The remainder of this paper is structured in the following manner: Sec. 2 gives details of the proposed design methods. This includes a review of the traditional CS and reweighted l_1 minimisation problems, along with our proposed robustness constraint and three design methods to enforce the minimum spacing constraint. In Sec. 3 multiband design examples are presented and compared with a GA based design method. Finally conclusions are drawn in Sec. 4.

2 Proposed Design Method

2.1 Array Model

A narrowband array structure consisting of M antennas is shown in Fig. 1. The antennas are assumed to be omnidirectional with identical responses. Also shown are the received array signals, $x_m[n]$, for $m = 1, 2, \ldots, M$, with a desired signal arriving at an angle of θ. A plane-wave signal model is assumed, i.e. the signal impinges upon the array from the far field. The distance from the first antenna to subsequent antennas is denoted as d_m for $m = 1, 2, \ldots, M$, with $d_1 = 0$, i.e. the distance from the first antenna to itself.

The steering vector of the array is given by

$$\mathbf{s}(\Omega, \theta) = [1, e^{-j\mu_2 \Omega \cos \theta}, \ldots, e^{-j\mu_M \Omega \cos \theta}]^T, \tag{1}$$

where $\Omega = \omega T_s$ is the normalized frequency with T_s being the sampling period, $\mu_m = \frac{d_m}{cT_s}$ for $m = 1, 2, \ldots, M$, and $\{\cdot\}^T$ denotes the transpose operation.

The response of the array is then given by

$$p(\Omega, \theta) = \mathbf{w}^H \mathbf{s}(\Omega, \theta), \tag{2}$$

where $\mathbf{w}^H$ is the Hermitian transpose of the weight coefficient vector

$$\mathbf{w} = [\mathrm{w}_1 \quad \mathrm{w}_2 \quad \ldots \quad \mathrm{w}_M]^T. \tag{3}$$

3

2.2 Robust Sparse Array Design Method

CS can be used to design sparse arrays by trying to match the array's response to a desired/reference response $p_r(\Omega, \theta)$. First, consider Fig. 1 as being a grid of potential active antenna locations. In this instance, d_M is the aperture of the array and the values of d_m, for $m = 2, 3, \ldots, M - 1$, are selected to give a uniform grid, with M being a very large number. Sparseness is then introduced by selecting the weight coefficients to give as few active antennas as possible, while still giving a designed response that is close to the desired one.

This problem is first formulated as

$$
\begin{aligned}
\min \quad & ||\mathbf{w}||_0 \\
\text{subject to} \quad & ||\mathbf{p}_r - \mathbf{w}^H \mathbf{S}||_2 \leq \alpha
\end{aligned}
\tag{4}
$$

where $||\mathbf{w}||_0$ is the number of nonzero weight coefficients in $\mathbf{w}$, $\mathbf{p}_r$ is the vector holding the desired beam response at the sampled angular points θ_l, $l = 0, 1, \cdots, L - 1$, for the frequency of interest Ω, $\mathbf{S}$ is the matrix composed of the corresponding steering vectors and α places a limit on the allowed difference between the desired and the designed responses. In this constraint $|| \cdot ||_2$ denotes the l_2 norm. In detail, $\mathbf{p}_r$ and $\mathbf{S}$ are respectively given by

$$
\begin{aligned}
\mathbf{p}_r &= [p_r(\Omega, \theta_0), p_r(\Omega, \theta_1), \cdots, p_r(\Omega, \theta_{L-1})], \\
\mathbf{S} &= [\mathbf{s}(\Omega, \theta_0), \mathbf{s}(\Omega, \theta_1), \cdots, \mathbf{s}(\Omega, \theta_{L-1})].
\end{aligned}
$$

Here the desired response $p_r(\Omega, \theta)$ can be an ideal one, i.e. with a value of one at the mainlobe and zeros over the sidelobe region, or obtained from that of a traditional ULA design method. In our design examples and what follows we assume that the $p_r(\Omega, \theta)$ is an ideal response.

However, (4) is computationally expensive and the problem can be more efficiently expressed as a minimisation of the l_1 norm of the weight coefficients [16], i.e.

$$
\begin{aligned}
\min \quad & ||\mathbf{w}||_1 \\
\text{subject to} \quad & ||\mathbf{p}_r - \mathbf{w}^H \mathbf{S}||_2 \leq \alpha \ .
\end{aligned}
\tag{5}
$$

Then suppose that the actual steering vector is related to the assumed steering vector by $\tilde{\mathbf{s}} = \mathbf{s} + \mathbf{e}$, where $\mathbf{s}$ is the designed steering vector (given by (1)) and $\mathbf{e}$ is the error introduced by model perturbations. If this error is norm-bounded, i.e.

$$
||\mathbf{e}||_2 \leq \varepsilon,
\tag{6}
$$

where ε is the upper bound, then the possible difference between designed and achieved array response is given by

$$
|\mathbf{w}^H \tilde{\mathbf{s}} - \mathbf{w}^H \mathbf{s}| = |\mathbf{w}^H \mathbf{e}| \leq \varepsilon ||\mathbf{w}||_2.
\tag{7}
$$

We can then add this as an extra constraint to (5), leading to

$$\min \quad ||\mathbf{w}||_1$$
$$\text{subject to} \quad ||\mathbf{p}_r - \mathbf{w}^H \mathbf{S}||_2 \le \alpha$$
$$\varepsilon ||\mathbf{w}||_2 \le \beta, \tag{8}$$

where the second constraint ensures that the difference in array response, caused by the norm-bounded error, remains below a predetermined acceptable level specified by β. As a result, a robust sparse array against the norm-bounded errors is obtained.

Unlike the l_0 norm, the l_1 norm does not penalise all non-zero valued coefficients equally. Instead, larger coefficients are penalised more heavily. To further improve the sparseness of the array and get a better approximation of the l_0 norm minimisation, we can add smaller weighting terms to the larger elements w_m of the weight vector $\mathbf{w}$, so that smaller values in $\mathbf{w}$ are penalised more [27, 28, 29]. We can do this in an iterative way and change (8) into a reweighted minimisation problem as follows

$$\min \sum_{m=1}^{M} \delta_m^i |w_m^i| \text{ subject to } ||\mathbf{p}_r - \mathbf{w}_i^H \mathbf{S}||_2 \quad \le \quad \alpha$$
$$\varepsilon ||\mathbf{w}_i||_2 \quad \le \quad \beta, \tag{9}$$

where i is the current iteration, $\mathbf{w}_i = [w_1^i, w_2^i, \dots w_M^i]^T$ holds the current estimate of the weight coefficients, $\delta_m^i = (|w_m^{i-1}| + \gamma)^{-1}$ and γ is a small value roughly equal to the minimum desired weight coefficient. The iterative algorithm would then follow the steps below:

1. Set $i = 0$ and find an initial estimate of the weight coefficients $\mathbf{w}_i$ by solving (8).

2. $i = i + 1$, and find the reweighting terms δ_m^i.

3. Solve (9).

4. Repeat steps 2 to 3 until $||\mathbf{w}_i||_0 = ||\mathbf{w}_{i-1}||_0 = ||\mathbf{w}_{i-2}||_0$ i.e. until the number of active locations has remained the same for three iterations.

The addition of the reweighting term, which is calculated using coefficients from the previous iteration, means non-zero valued coefficients are penalised in a more uniform manner. A large coefficient in the previous iteration gives a small reweighting term, meaning the active location is likely to be replicated in the current iteration. However, a small coefficient value in the previous iteration gives a large reweighting term in the current iteration. As a result, the potential active location is more heavily penalised. This gives a better approximation of minimising the l_0 norm.

Both (8) and (9) can be solved using cvx, a package for specifying and solving convex programs [38, 39]. It is also possible to extend both to solve multiband design problems. To do this, $\mathbf{p}_r$ and $\mathbf{S}$ can be specified in
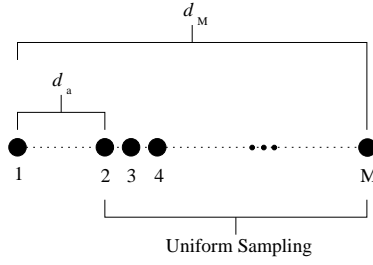
Figure 2: Sampling of potential antenna locations.

the following way

$$
\begin{aligned}
\mathbf{p}_r \;=\; & [p_r(\Omega_0, \theta_0), \cdots, p_r(\Omega_0, \theta_{L-1}), \cdots, \\
& p_r(\Omega_{F-1}, \theta_0), \cdots, p_r(\Omega_{F-1}, \theta_{L-1})],
\end{aligned}
$$

and

$$
\begin{aligned}
\mathbf{S} \;=\; & [\mathbf{s}(\Omega_0, \theta_0), \cdots, \mathbf{s}(\Omega_0, \theta_{L-1}), \cdots, \\
& \mathbf{s}(\Omega_{F-1}, \theta_0), \cdots, \mathbf{s}(\Omega_{F-1}, \theta_{L-1})],
\end{aligned}
$$

where F frequencies of interest are being considered and $p_r(\Omega_f, \theta_l)$ and $\mathbf{s}(\Omega_f, \theta_l)$ are the desired response and steering vector for the fth frequency Ω_f at the lth angular point θ_l respectively.

2.3 Solutions to the Physical Size Problem

However, the solutions to (8) and (9) can lead to active locations that are too close together, which may become impractical due to the antennas not fitting in the specified locations. As a result, a minimum adjacent antenna separation of the antennas' physical size has to be enforced. Three proposed methods of doing so are detailed below.

2.3.1 Post Processing Method

A straightforward method is to merge the resultant locations which are too close to each other. However, it is not difficult to modify the standard design methods in (8) and (9) to make sure that if needed at least the first two active antennas have a large enough spacing.

Assume the size of the antenna is d_a and the allowed maximum aperture for the array is d_M. Then instead of sampling the distance d_M uniformly with M potential antenna locations, we choose the first two locations with a distance d_a as shown in Fig. 2.

First use (8) or (9) to obtain the initial active locations. If the first location is included in the initial result, then the second active antenna location will be at least a distance of d_a away from it according to the sampling scheme in Fig. 2.
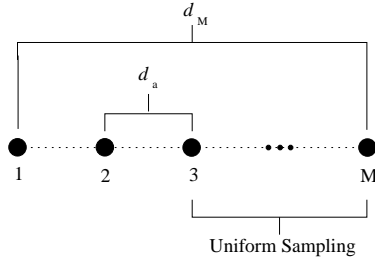
6

Figure 3: Sampling of potential antenna locations, where locations 1 and 2 are final active locations obtained by the procedure in Sec. 2.3.1.

Now to decide the second active location, we first find the next cluster of initial active locations with an adjacent spacing less than d_a. Then we take the average of the clustered locations as the second active location. Note that when we form this cluster of initial active locations, we need to ensure the distance from the first to last locations of the cluster is less than d_a, otherwise we need to split the cluster into at least two sub-clusters so that we can fit at least two antennas into this distance instead of one (if only one whole cluster is considered). In the same way we then find the remaining active antenna locations. Obviously, we will not be able to obtain the optimal solution using this method. However, we will see in our design examples that a satisfactory design result can still be obtained.

2.3.2 Iterative Minimum Distance Sampling Method

This method is a further modification of the post-processing method described in Sec. 2.3.1. After finding the first active location (location 1 in Fig. 2) and the second one (through merging the first cluster of active locations) according to the procedure in Sec. 2.3.1, we sample the aperture between location 3 and location M uniformly with the distance between location 2 and location 3 being d_a as shown in Fig. 3.

Now using the design method (8) or (9), we can obtain the initial active locations between location 2 and M in Fig. 3. Then following the post-processing procedure we can find the third final active location.

Fixing the first, second and third active locations, uniformly sampling between location 4 and M, where the distance between location 4 and location 3 is d_a, we obtain another set of initial active antenna locations. Repeat this process until the remaining range is less than the size of the antenna.

2.3.3 Reweighted Method

In order to enforce the size constraint and exploit the extra sparsity of the reweighted l_1 minimisation problem, the reweighting scheme in (9) is changed to

$$
\delta_m^i = \begin{cases} (|w_m^{i-1}| + \gamma)^{-1} & m = 1 \\ (|w_m^{i-1}| + \gamma)^{-1} & m > 1 \text{ and constraint met} \\ (\gamma)^{-1} & \text{otherwise.} \end{cases} \tag{10}
$$

Now instead of repeating the iterative process (detailed in Sec. 2.2) until the number of active locations has remained the same for three iterations, the process is continued until the size constraint is enforced.

Unfortunately this algorithm will not always guarantee a viable solution, due to the presence of γ in the calculation of reweighting terms. The inclusion of γ is required for numerical stability, but prevents a zero weight coefficient in the current iteration guaranteeing a zero weight coefficient in the next iteration. However, based on our experience with different design parameters, if a solution is possible it will usually be achieved in approximately 5 iterations.

The basic framework of the l_1 minimisation problem in our proposed design methods follows that of previous CS based work. As a result it would be reasonable to assume that a solution will be guaranteed in majority of cases that the previous work does. However, the addition of enforcing the size constraint and the iterative nature of the iterative minimum sampling and reweighted methods means that in some cases a solution may not be reached. In the case of the iterative minimum sampling method it is also possible that the method could fail at a given iteration. However, it would still be possible to get a suitable solution by applying the post processing method to the active antenna locations found in the previous iteration.
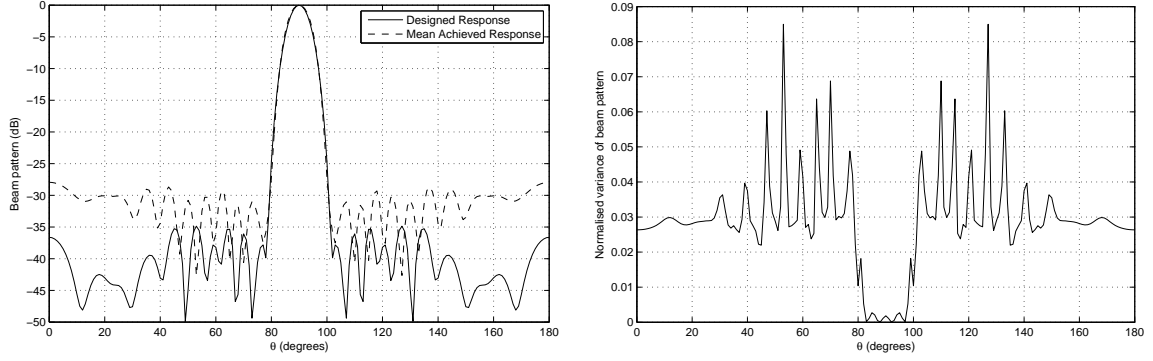
3 Design Examples

In this section narrowband and multiband design examples are presented to verify the effectiveness of the proposed design methods. The design examples were all implemented on a computer with an Intel Core Duo CPU E6750 (2.66GHz) and 4GB of RAM.

The average achieved response and variance of responses are calculated when assessing the robustness of an array. When doing so $N = 1000$ different error vectors are generated that meet the condition given in (6). For the nth error vector the achieved response at angle θ_k, $p_n(\theta_k)$, is found and the average achieved response is given by

$$
\bar{p}(\theta_k) = \frac{1}{N} \sum_{n=0}^{N-1} p_n(\theta_k), \tag{11}
$$

which is then used to find the normalised variance of the achieved array response,

$$
var(\theta_k) = \frac{1}{N} \sum_{n=0}^{N-1} \frac{|p_n(\theta_k) - \bar{p}(\theta_k)|^2}{|\bar{p}(\theta_k)|}, \tag{12}
$$

(a) Responses for the narrowband post-processing design example. (b) Normalised variance for the narrowband post-processing design example.

Figure 4: Narrowband design results for the post-processing method.

A close match between mean achieved and designed responses, along with low normalised variance levels, would indicate that robustness has been achieved.

For all design examples antenna locations with negligible contributions (coefficient values below 1×10^{-3}) to the overall response were discarded and some degree of location merger was required. As a result the final weight coefficients may no longer be optimal for the final antenna locations. However, the locations will allow the effective design of a robust beamformer using the formulation as detailed in [10]. The same method is also used to find the coefficients for the comparison GA design examples. In both cases the same values of α and β (note that α and β here are not the same variables as in the CS-based design methods) are selected when finding the optimal weight coefficients, in order to allow a fair comparison.

3.1   Narrowband Examples

First the CS-based design methods were used to design a sparse array over a potential aperture of 15λ, where λ is the wavelength of the signal of interest with normalised frequency $\Omega = \pi$. This aperture was split into a grid of 300 potential active antenna locations and each antenna assumed to have a size of 0.8λ. The desired main-lobe is set to the single point of $\theta_{ML} = 90°$ with the sidelobe regions set as $\theta_{SL} = [0°, 80°] \bigcup [100°, 180°]$ being sampled every $1°$. The values of $\alpha = 0.75$ and $\beta = 0.4$ were placed on the constraints in the optimisations and the value $\epsilon = 1$ also used. After the discarding and merging of initial locations, the (separate from previous mentioned) values of $\alpha = 0.8$ and $\beta = 0.01$ were used in the redesigning of the weight coefficients.

The post-processing method resulted in 17 active antenna locations as detailed in Table. 1. Figs. 4(a) and 4(b) show the responses and variance level, respectively. It can be seen that both the designed and mean achieved responses are at the desired location of $\theta = 90°$. There is also sufficient sidelobe attenuation and a reasonable match between designed and mean achieved responses. Along with the low normalised variance levels this again suggests that some degree of robustness has been achieved successfully. It is also clear that the size constraint has been met.

9

Table 1: Antenna locations for the narrowband post-processing design example.

n	d_n/λ	n	d_n/λ
1	0	10	8.45
2	0.8	11	6.69
3	1.88	12	9.25
4	2.76	13	10.06
5	4.41	14	11.26
6	5.22	15	12.55
7	6.02	16	13.39
8	6.83	17	14.61
9	7.64		

Table 2: Antenna locations for the narrowband iterative design example.

| n	d_n/λ	n	d_n/λ
1	0	10	7.94
2	0.8	11	8.79
3	1.98	12	9.70
4	2.80	13	10.50
5	3.66	14	11.39
6	4.51	15	12.29
7	5.38	16	13.28
8	6.22	17	14.32
9	7.10		

The iterative method also resulted in 17 active antenna locations as detailed in Table. 2. Fig. 5(a) shows the designed and mean achieved array responses and Fig. 5(b) shows the normalised variance level. The reweighted method resulted in 13 active antenna locations as detailed in Table. 3. Fig. 6(a) and 6(b) show the corresponding results. Similar observations for both methods can be obtained as in the case of the post-processing method, i.e. satisfactory design results have been achieved.

For the GA comparison design example, the values $\alpha = 0.8$ and $\beta = 0.01$ were again used. A population of 60 individuals was used, creating 54 offspring in each of the 100 generations. In addition, a mutation rate of 0.4 was also used. The resulting antenna locations are shown in Table. 4 with the resulting responses and variance being shown in Figs. 7(a) and 7(b), respectively.

For the designed response the mainlobe is in the required location, with sufficient sidelobe attenuation also being achieved. There is also a good match between designed and mean achieved responses around
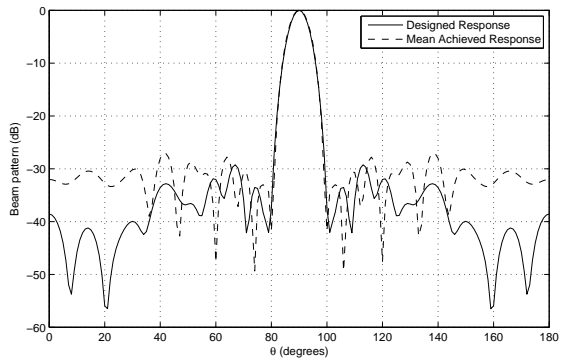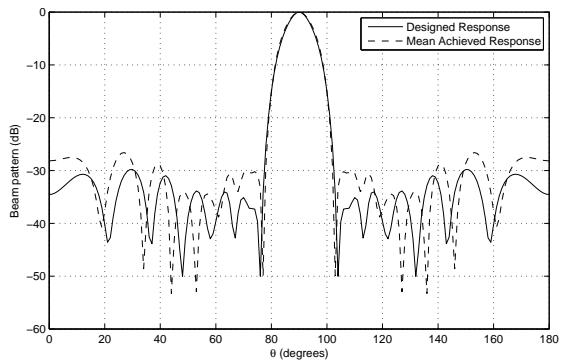
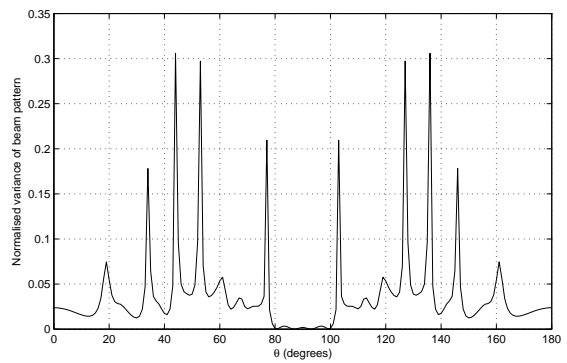(a) Responses for the narrowband iterative design example.
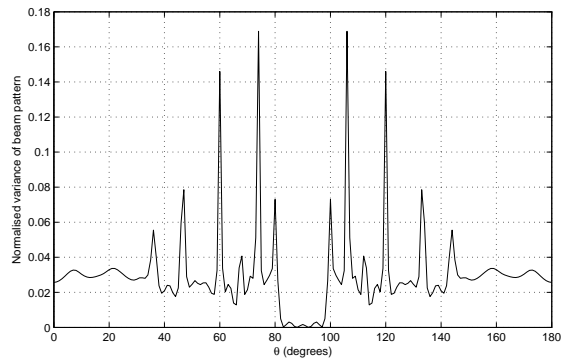
(b) Normalised variance for the narrowband iterative design example.

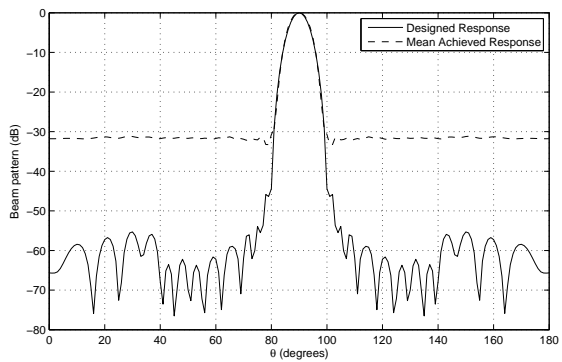Figure 5: Narrowband design results for the iterative method.

(a) Responses for the narrowband reweighted design example.
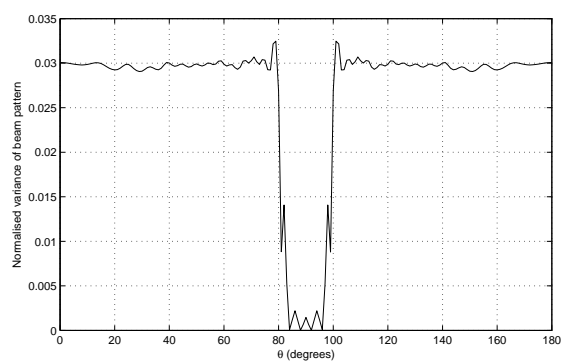
(b) Normalised variance for the narrowband reweighted design example.

Figure 6: Narrowband design results for the reweighted method.

(a) Responses for the narrowband GA design example.

(b) Normalised variance for the narrowband GA design example.

Figure 7: Narrowband design results for the GA method.

Table 3: Antenna locations for the narrowband reweighted design example.

n	d_n/λ	n	d_n/λ
1	1.61	8	7.22
2	2.41	9	8.13
3	3.21	10	10.84
4	4.01	11	11.69
54	4.82	12	12.54
6	5.62	13	13.39
7	6.42		

Table 4: Antenna locations for the narrowband GA design example.

n	d_n/λ	n	d_n/λ
1	0	10	8.21
2	1.77	11	9.01
3	2.58	12	9.81
4	3.38	13	10.61
5	4.19	14	11.41
6	5.00	15	12.21
7	5.80	16	13.01
8	6.61	17	14.61
9	7.41		

the mainlobe. Although the mean achieved response does not match the designed response as well, in the sidelobe regions sufficient attenuation has been achieved. Along with the low variance levels this indicates an acceptable performance in terms of robustness has been achieved. It is possible that a better match between the two responses in the sidelobe regions could also be achieved by increasing the population size or the number of allowed generations. However, this has the effect of drastically increasing the computation time, which would not be desirable.

To compare the performance of the four methods in a quantitative way, we consider the following criteria: the number of active antennas (or $||\mathbf{w}||_0$), the aperture length, the mean adjacent antenna separation, $||\mathbf{p}_r - \mathbf{w}^H \mathbf{S}||_2$, $\varepsilon||\mathbf{w}||_2$, and finally, the computation time. Table. 5 summarises the results for the various design examples, where all values are found using the optimal weight coefficients for the final active antenna locations.

Firstly we can clearly see the main advantage of the CS-based methods, i.e. a considerable decrease in the computation time. We would see this irrespective of which CS-based method was selected for comparison

Table 5: Summary of performance measures for the proposed methods and a GA (narrowband).

Method	Post-Pro	Iterative	Reweighted	GA
$||\mathbf{w}||_0$	17	17	13	17
Aperture/λ	14.61	14.32	11.79	14.61
Mean Separation/λ	0.91	0.90	0.98	0.91
$||\mathbf{p}_r - \mathbf{w}^H\mathbf{S}||_2$	0.1546	0.1897	0.3626	0.0179
$\varepsilon||\mathbf{w}||_2$	0.3367	0.3138	0.3301	0.3136
Computation time (seconds)	4.84	80.00	8.21	12664.04

with the GA.

We can also see that all of the design methods have provided a suitably sparse array. In each case the mean adjacent antenna separation is larger than $\lambda/2$ and less active antennas are required compared to an equivalent ULA with a spacing of $\lambda/2$.

The values of $||\mathbf{p}_r - \mathbf{w}^H\mathbf{S}||_2$ show that in this case the three proposed design methods have not managed to match the desirability of the response found using the GA. However, as shown in the figures, they are at an acceptable level and we need to bear in mind that they are achieved in a considerably shorter computation time.

Comparing the values of $\varepsilon||\mathbf{w}||_2$, we can see that the three proposed design methods have performed comparably to the GA in terms of robustness to steering vector error.
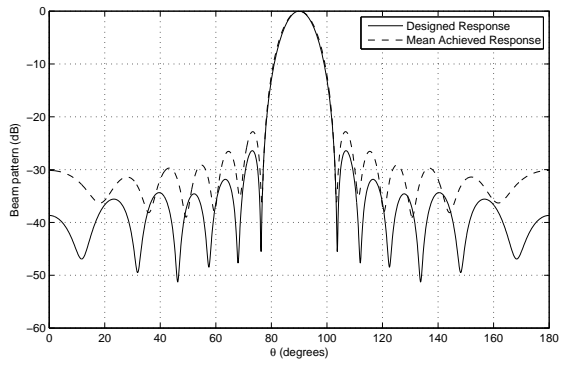
3.2 Multiband Examples

In this instance we first find a multiband GA comparison design example with the values $\alpha = 0.8$ and $\beta = 0.01$ being used. Two frequency bands are now considered, one with a normalised frequency of $\Omega_1 = 0.75\pi$ and a second with a normalised frequency of $\Omega_2 = \pi$. We looked to design an array consisting of 12 0.8λ-sized antennas spread over an aperture of 10λ, where λ is the wavelength relating to a normalised frequency of π. The desired mainlobe is set to the single point of $\theta_{ML} = 90°$ with the sidelobe regions set as $\theta_{SL} = [0°, 80°] \bigcup [100°, 180°]$ being sampled every $1°$. A population of 60 individuals was used in the GA-based design method, creating 54 offspring in each of the 100 generations. In addition a mutation rate of 0.4 was used and the value of ε set to 1.

The resulting antenna locations are shown in Table. 6 with the resulting responses for the first and second frequencies of interest being shown in Figs. 8(a) and 8(b), respectively. Fig. 8(c) shows the normalised variance levels for the GA design example.
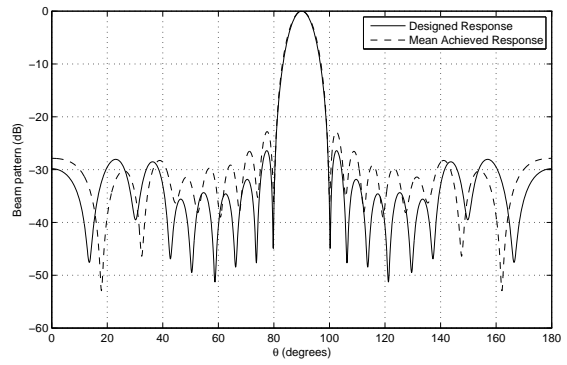
For both frequencies of interest the mainlobe is in the correct location for the designed and mean achieved

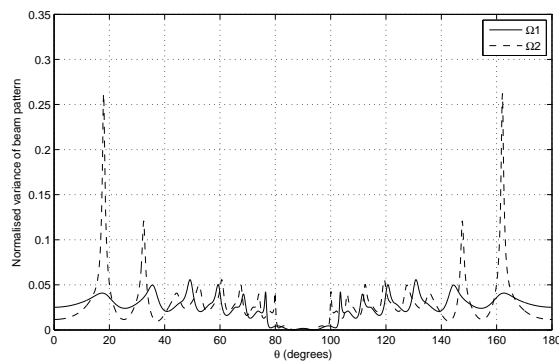Table 6: Antenna locations for the multiband GA design example.

n	d_n/λ	n	d_n/λ
1	0	7	5.19
2	1.10	8	6.00
3	1.92	9	6.81
4	2.73	10	7.61
5	3.55	11	8.41
6	4.37	12	10

(a) Responses for the multiband GA design example at normalised frequency $\Omega_1 = 0.75\pi$.

(b) Responses for the multiband GA design example at normalised frequency $\Omega_1 = \pi$.

(c) Normalised variances for the multiband GA design example.

Figure 8: Multiband design results for the GA method.

Table 7: Antenna locations for the multiband post-processing design example.

n	d_n/λ	n	d_n/λ
1	0	7	5.86
2	1.41	8	6.69
3	2.49	9	7.57
4	3.32	10	8.41
5	4.15	11	9.49
6	5.03		

responses, and there is sufficient sidelobe attenuation, with a reasonable match between designed and mean achieved responses. It is also clear that the resulting antenna locations meet the constraint of the antenna's size for the minimum adjacent antenna separation.

To have a better comparison between the CS-based methods and the GA, the values of $||\mathbf{p}_r - \mathbf{w}^H\mathbf{S}||_2$ and $\varepsilon||\mathbf{w}||_2$ are found for the resulting locations and weight coefficients using the GA and then set as the values of α and β in the CS-based design respectively. This gives us values of $\alpha = 0.6984$ and $\beta = 0.3038$. For the CS-based methods we consider a grid of 200 potential active antenna locations uniformly spread over the distance being sampled.

The post-processing method resulted in 11 active antenna locations as detailed in Table. 7. Figs. 9(a) and 9(b) show the designed and mean achieved array responses for the two frequencies, with Fig. 9(c) giving the normalised variance levels.

It can be seen that for both frequencies of interest both the designed and mean achieved responses are at the desired location of $\theta = 90°$. There is also sufficient sidelobe attenuation and a reasonable match between designed and mean achieved responses. Along with the low normalised variance levels this again suggests that some degree of robustness has been achieved successfully. It is also clear that the size constraint has been met.

The iterative method resulted in 11 active antenna locations as detailed in Table. 8. Figs. 10(a) and 10(b) show the designed and mean achieved array responses and Fig. 10(c) shows the normalised variance levels. The reweighted method resulted in 12 active antenna locations as detailed in Table. 9. Figs. 11(a), 11(b) and 11(c) show the corresponding results. Similar observations for both methods can be obtained as in the case of the post-processing method, i.e. satisfactory design results have been achieved.

To compare their performance in a quantitative way, we again consider the following criteria: the number of active antennas (or $||\mathbf{w}||_0$), the aperture length, the mean adjacent antenna separation, $||\mathbf{p}_r - \mathbf{w}^H\mathbf{S}||_2$, $\varepsilon||\mathbf{w}||_2$, and the computation time. Table. 10 summarises the results, where all values are found using the optimal weight coefficients for the final active antenna locations.

Firstly, the main advantage of the CS-based methods can easily be seen again, i.e. a much shorter computation time. This is especially true for the post-processing method, where only a single l_1 minimisation is
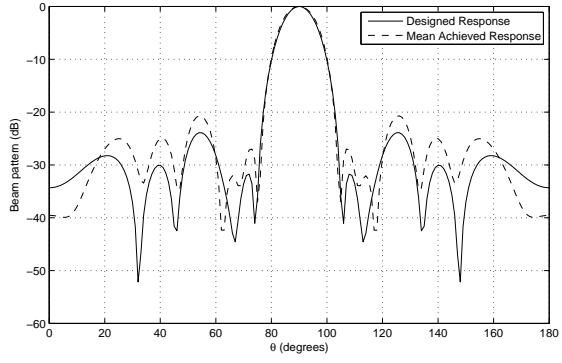
(a) Responses for the multiband post-processing design example at normalised frequency $\Omega_1 = 0.75\pi$.
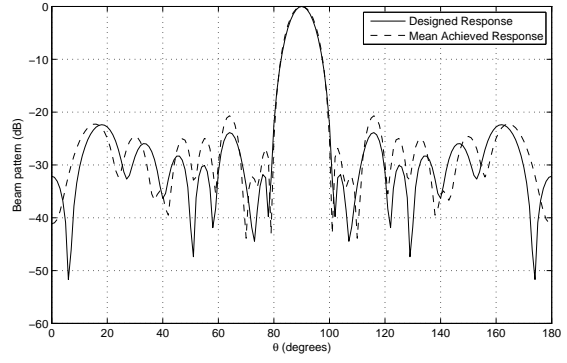
(b) Responses for the multiband post-processing design example at normalised frequency $\Omega_1 = \pi$.
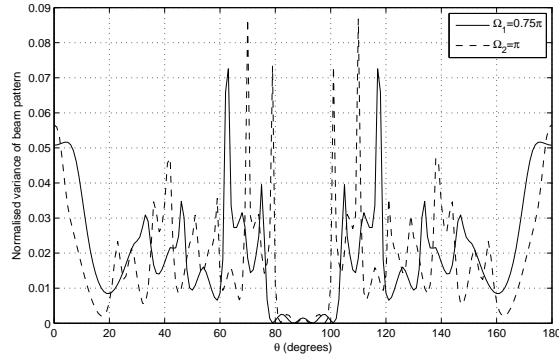
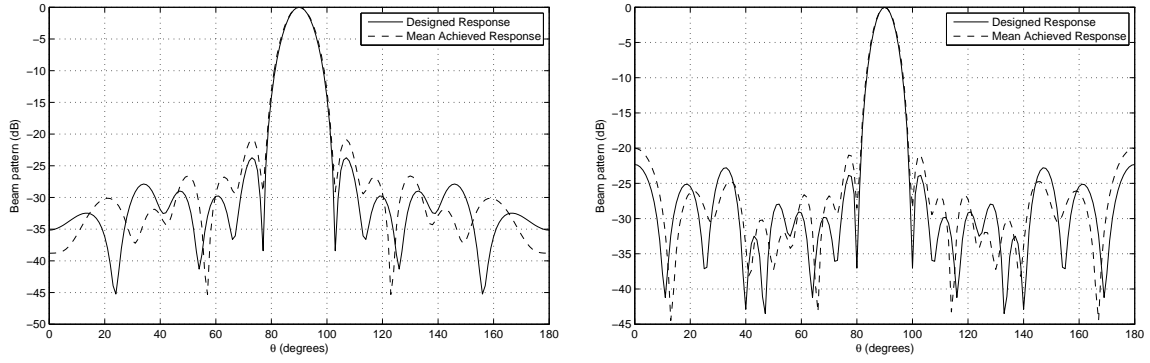(c) Normalised variances for the multiband post-processing design example.

Figure 9: Multiband design results for the post-processing method.

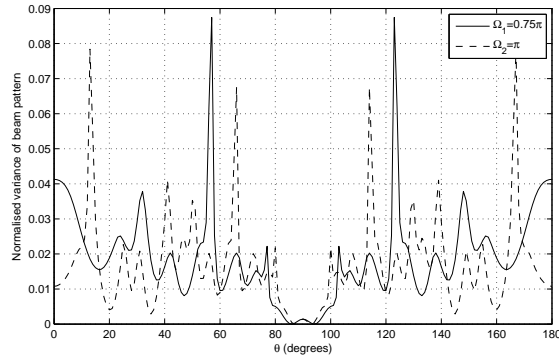Table 8: Antenna locations for the multiband iterative design example.

n	d_n/λ	n	d_n/λ
1	0	7	5.47
2	1.19	8	6.34
3	2.01	9	7.20
4	2.87	10	8.07
5	3.72	11	9.23
6	4.62		

(a) Responses for the multiband iterative design example at normalised frequency $\Omega_1 = 0.75\pi$.

(b) Responses for the multiband iterative design example at normalised frequency $\Omega_1 = \pi$.

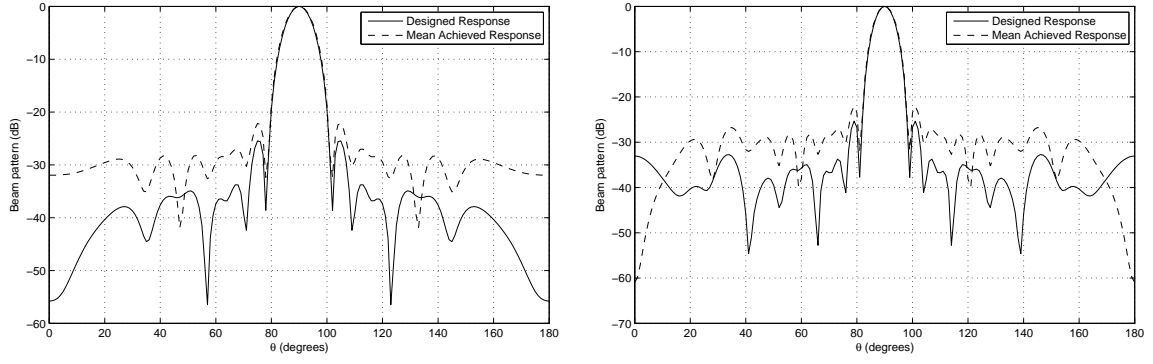(c) Normalised variances for the multiband iterative design example.

Figure 10: Multiband design results for the iterative method.

Table 9: Antenna locations for the multiband reweighted design example.

n	d_n/λ	n	d_n/λ
1	0.80	7	5.83
2	1.61	8	6.68
3	2.41	9	7.54
4	3.27	10	8.34
5	4.12	11	9.20
6	4.97	12	10

(a) Responses for the multiband reweighted design example at normalised frequency $\Omega_1 = 0.75\pi$.

(b) Responses for the multiband reweighted design example at normalised frequency $\Omega_1 = \pi$.

(c) Normalised variances for the multiband reweighted design example.

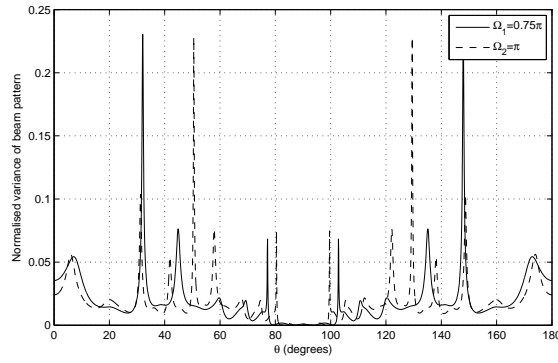Figure 11: Multiband design results for the reweighted method.

Table 10: Summary of performance measures for the proposed methods and a GA.

Method	GA	Post-pro	Iterative	Reweighted
$||\mathbf{w}||_0$	12	11	11	12
Aperture$/\lambda$	10	9.49	9.23	9.2
Mean Separation$/\lambda$	0.91	0.95	0.92	0.84
$||\mathbf{p}_r - \mathbf{w}^H\mathbf{S}||_2$	0.6984	1.0466	0.9024	0.4590
$\varepsilon||\mathbf{w}||_2$	0.3038	0.2784	0.2855	0.3084
Computation time (seconds)	1459.39	7.05	28.71	12.65

required.

The CS-based methods also give a comparable performance in terms of the level of sparsity that is introduced. We can see that although the post-processing and iterative minimum distance sampling methods result in less active antennas, compared to the GA, there is also a shorter aperture. As a result, the mean adjacent antenna separation is roughly the same. For the reweighted design example the resulting array has the same number of active antennas but over a shorter aperture. As a result, the mean adjacent separation is less than for the GA. However, it is still larger than the maximum adjacent separation possible for an equivalent ULA.

The values of $||\mathbf{p}_r - \mathbf{w}^H\mathbf{S}||_2$ indicate that the desirability of the designed response is not as good for the post-processing and iterative minimum distance sampling methods compared to the GA method. A potential reason for this is the fact that some antenna locations have been clustered together and merged in both cases. Another reason, which may be more important, is that in both cases the aperture of the resultant array is smaller than the GA result. However, we can also see that the designed response for the reweighted method looks more desirable than the GA design method, although it has the smallest aperture among the four.

The values of $\varepsilon||\mathbf{w}||_2$ show a comparable performance is achieved in terms of the array's robustness to steering vector error. Only the reweighted method performs slightly worse than the GA method, while still preserving an acceptable level of robustness. This is also due to the trade-off between the values of $||\mathbf{p}_r - \mathbf{w}^H\mathbf{S}||_2$ and $\varepsilon||\mathbf{w}||_2$ since the reweighted method gives the best desirability result.

As a result of the comparable (to GA) or reasonable performance levels of the three proposed methods we can say they are a valid alternative to previously established GA-based design method. Although the performance levels in some criteria may not always be as good as with a GA, each method will always be expected to give a reasonable level of sparsity in a much shorter period of time. If a further performance improvement is still required, the CS-based designed arrays could then be put into the initial population of a smaller GA problem (i.e. less generations should be required as a good solution is provided in the initial population).

Finally, it is worth noting that some of the adjacent antenna separations for each design method can get close to the minimum of the size constraint. In some cases this may introduce strong mutual coupling, degrading the performance of the array. This extreme case could be avoided by introducing the concept of a virtual antenna with a larger size than the physical antenna. For example, for an antenna with a physical size of 0.8λ the size constraint could be enforced to a virtual size of 1λ, therefore increasing the minimum adjacent antenna separations.

4 Conclusions

In this paper, three design methods have been proposed for the design of robust sparse antenna arrays. All of the methods are based on compressive sensing and enforce a constraint of the antenna's size on the minimum

adjacent antenna separation. Robustness is achieved by adding an extra constraint to the compressive sensing problem. This constraint keeps the discrepancy between designed and mean achieved array responses, due to a norm-bounded steering vector error, below a predefined acceptable level. The first method of enforcing the size constraint is mainly to merge locations that are closer together than the size constraint. The second method looks at iteratively finding active antenna locations through a minimum distance sampling scheme in the design, while the third method is based on a reweighted l_1 norm minimisation scheme, where the stopping criteria is changed to when the size constraint has been met. Narrowband and multiband design examples have been shown to verify the effectiveness of the three proposed design methods with comparisons being drawn with a genetic algorithm based design method. Although it is possible for genetic algorithms to give a better result in terms of some specific criteria, it is not guaranteed in every case and takes a considerably long time compared to our proposed designs. Overall, we can say the compressive sensing based design methods are a valid alternative to genetic algorithm based design methods.

References

[1] H. L. Van Trees, *Optimum Array Processing, Part IV of Detection, Estimation, and Modulation Theory*. New York, U.S.A.: John Wiley & Sons, Inc., 2002.

[2] W. Liu and S. Weiss, *Wideband Beamforming: Concepts and Techniqeus*. Chichester, UK: John Wiley & Sons, 2010.

[3] D. G. Bodnar, B. Keither Rainer, and Y. Rahmat-Samii, "A novel array antenna for MSAT applications," *IEEE Transactions on Vehicular Technology*, vol. 38, no. 2, pp. 86–94, May 1989.

[4] S. Choi, J. Choi, H. Im, and B. Choi, "A novel adaptive beamforming algorithm for antenna array CDMA systems with strong interferers," *IEEE Transactions on Vehicular Technology*, vol. 51, no. 5, pp. 808–816, September 2002.

[5] P. Jarske, T. Saramaki, S. K. Mitra, and Y. Neuvo, "On properties and design of nonuniformly spaced linear arrays," *IEEE Transactions on Acoustics, Speech, and Signal Processing*, vol. 36, no. 3, pp. 372–380, March 1988.

[6] R. L. Haupt, "Thinned arrays using genetic algorithms," *IEEE Transactions on Antennas and Propagation*, vol. 42, no. 7, pp. 993–999, July 1994.

[7] K.-K. Yan and Y. Lu, "Sidelobe reduction in array-pattern synthesis using genetic algorithm," *IEEE Transactions on Antennas and Propagation*, vol. 45, no. 7, pp. 1117 –1122, July 1997.

[8] K. Chen, Z. He, and C. Han, "Design of 2-dimensional sparse arrays using an improved genetic algorithm," in *Proc. IEEE Workshop on Sensor Array and Multichannel Processing*, July 2006, pp. 209–213.

[9] L. Cen, W. Ser, Z. L. Yu, and S. Rahardja, "An improved genetic algorithm for aperiodic array synthesis," in *Proc. IEEE International Conference on Acoustics, Speech, and Signal Processing*, April 2008, pp. 2465 –2468.

[10] M. Hawes and W. Liu, "Location optimization of robust sparse antenna arrays with physical size constraint," *IEEE Antennas and Wireless Propagation Letters*, vol. 11, pp. 1303 –1306, 2012.

[11] A. Trucco and V. Murino, "Stochastic optimization of linear sparse arrays," *IEEE Journal of Oceanic Engineering*, vol. 24, no. 3, pp. 291–299, July 1999.

[12] G. Oliveri, M. Donelli, and A. Massa, "Linear array thinning exploiting almost difference sets," *IEEE Transactions on Antennas and Propagation*, vol. 57, no. 12, pp. 3800–3812, 2009.

[13] G. Oliveri, L. Manica, and A. Massa, "Ads-based guidelines for thinned planar arrays," *IEEE Transactions on Antennas and Propagation*, vol. 58, no. 6, pp. 1935–1948, 2010.

[14] S. Caorsi, A. Lommi, A. Massa, and M. Pastorino, "Peak sidelobe level reduction with a hybrid approach based on gas and difference sets," *IEEE Transactions on Antennas and Propagation*, vol. 52, no. 4, pp. 1116–1121, 2004.

[15] G. Oliveri and A. Massa, "Genetic algorithm (ga)-enhanced almost difference set (ads)-based approach for array thinning," *IET Microwaves Antennas Propagation*, vol. 5, no. 3, pp. 305–315, 2011.

[16] E. Candes, J. Romberg, and T. Tao, "Robust uncertainty principles: exact signal reconstruction from highly incomplete frequency information," *IEEE Transactions on Information Theory*, vol. 52, no. 2, pp. 489 – 509, February 2006.

[17] L. Li, W. Zhang, and F. Li, "The design of sparse antenna array," *CoRR*, vol. arXiv.org/abs/0811.0705, 2008.

[18] G. Prisco and M. D'Urso, "Exploiting compressive sensing theory in the design of sparse arrays," in *Proc. IEEE Radar Conference*, May 2011, pp. 865 –867.

[19] L. Carin, "On the relationship between compressive sensing and random sensor arrays," *IEEE Antennas and Propagation Magazine*, vol. 51, no. 5, pp. 72 –81, October 2009.

[20] L. Cen, W. Ser, W. Cen, and Z. L. Yu, "Linear sparse array synthesis via convex optimization," in *Proc. IEEE International Symposium on Circuits and Systems*, May 2010, pp. 4233–4236.

[21] M. B. Hawes and W. Liu, "Robust sparse antenna array design via compressive sensing," in *Proc. International Conference on Digital Signal Processing*, 2013.

[22] ——, "Sparse microphone array design for wideband beamforming," in *Proc. International Conference on Digital Signal Processing*, 2013.

[23] S. Ji, Y. Xue, and L. Carin, "Bayesian compressive sensing," *IEEE Transactions on Signal Processing*, vol. 56, no. 6, pp. 2346–2356, 2008.

[24] G. Oliveri and A. Massa, "Bayesian compressive sampling for pattern synthesis with maximally sparse non-uniform linear arrays," *Antennas and Propagation, IEEE Transactions on*, vol. 59, no. 2, pp. 467–481, 2011.

[25] G. Oliveri, M. Carlin, and A. Massa, "Complex-weight sparse linear array synthesis by bayesian compressive sampling," *IEEE Transactions on Antennas and Propagation*, vol. 60, no. 5, pp. 2309–2326, 2012.

[26] F. Viani, G. Oliveri, and A. Massa, "Compressive sensing pattern matching techniques for synthesizing planar sparse arrays," *IEEE Transactions on Antennas and Propagation*, vol. 61, no. 9, pp. 4577–4587, 2013.

[27] E. Candes, M. Wakin, and S. Boyd, "Enhancing sparsity by reweighted l_1 minimization," *Journal of Fourier Analysis and Applications*, vol. 14, no. 5-6, pp. 877–905, 2008.

[28] B. Fuchs, "Synthesis of sparse arrays with focused or shaped beampattern via sequential convex optimizations," *IEEE Transactions on Antennas and Propagation*, vol. 60, no. 7, pp. 3499 –3503, july 2012.

[29] G. Prisco and M. D'Urso, "Maximally sparse arrays via sequential convex optimizations," *IEEE Antennas and Wireless Propagation Letters*, vol. 11, pp. 192 –195, 2012.

[30] S. A. Vorobyov, A. B. Gersham, and Z. Q. Luo, "Robust adaptive beamforming using worst-case performance optimization: A solution to the signal mismatch problem," *IEEE Transactions on Signal Processing*, vol. 51, no. 2, pp. 313–324, February 2003.

[31] J. Li, P. Stoica, and Z. Wang, "On robust capon beamforming and diagonal loading," *IEEE Transactions on Signal Processing*, vol. 51, no. 7, pp. 1702–1715, July 2003.

[32] L. Lei, J. P. Lie, A. B. Gershman, and C. M. S. See, "Robust adaptive beamforming in partly calibrated sparse sensor arrays," *IEEE Transactions on Signal Processing*, vol. 58, no. 3, pp. 1661 –1667, march 2010.

[33] L. Yu, W. Liu, and R. J. Langley, "Novel robust beamformers for coherent interference suppression with DOA estimation errors," *IET Microwaves, Antennas and Propagation*, vol. 4, pp. 1310–1319, September 2010.

[34] Y. Zhao and W. Liu, "Robust wideband beamforming with frequency response variation constraint subject to arbitrary norm-bounded error," *IEEE Transactions on Antennas and Propagation*, no. 5, pp. 2566–2571, May 2012.

[35] L. Zhang and W. Liu, "Robust beamforming for coherent signals based on the spatial-smoothing technique," *Signal Processing*, vol. 92, pp. 2747–2758, November 2012.

[36] Y. Zhao and W. Liu, "Robust fixed frequency invariant beamformer design subject to norm-bounded errors," *IEEE Signal Processing Letters*, vol. 20, pp. 169–172, February 2013.

[37] C. C. Chen, B. A. Kramer, and J. L. Volakis, "Considerations on size reduction of UWB antennas," in *Proc. IEEE International Symposium on Antennas and Propagation*, June 2007, pp. 6011 –6014.

[38] C. Research, "CVX: Matlab software for disciplined convex programming, version 2.0 beta," *http://cvxr.com/cvx*, September 2012.

[39] M. Grant and S. Boyd, "Graph implementations for nonsmooth convex programs," in *Recent Advances in Learning and Control*, ser. Lecture Notes in Control and Information Sciences, V. Blondel, S. Boyd, and H. Kimura, Eds.   Springer-Verlag Limited, 2008, pp. 95–110.